Reduced scale model testing for prediction of eigenfrequencies and hydro-acoustic resonances in hydropower plants operating in off-design conditions

IOP Conf. Series: Earth and Environmental Science **240** (2019) 022022 doi:10.1088/1755-1315/240/2/022022

Reduced scale model testing for prediction of eigenfrequencies and hydro-acoustic resonances in hydropower plants operating in off-design conditions

A Favrel[1], **J Gomes Pereira Junior**[1], **C Landry**[2], **S Alligné**[2], **C Nicolet**[2], **F Avellan**[1]

[1] Ecole Polytechnique Fédérale de Lausanne, Avenue de Cour 33bis, Lausanne, Switzerland
[2] Power Vision Engineering Sàrl, Ecublens, Switzerland

email: arthur.favrel@epfl.ch

Abstract. The massive penetration of the electrical network by renewable energy sources, such as wind and solar, pushes the operators to extend hydropower plant units operating range to meet the transmission system operator requirements. However, in off-design operating conditions, flow instabilities are developing in Francis turbines, inducing cavitation, pressure pulsations and potentially resonance that can threaten the stability of the whole system. Reduced scale model testing is commonly performed to assess the hydraulic behaviour of the machine for industrial projects. However, it is not possible to directly transpose pressure pulsations and resonance conditions from model to prototype since the characteristics of the hydraulic circuits are different from model to prototype. In this paper, a methodology developed in the framework of the HYPERBOLE European research project for predicting the eigenfrequencies of hydropower plant units operating in off-design conditions is introduced. It is based on reduced scale model testing and proper one-dimensional modelling of the hydraulic circuits, including the draft tube cavitation flow, at both the model and prototype scales. The hydro-acoustic parameters in the draft tube are identified at the model scale for a wide number of operating conditions and, then, transposed to the full-scale machine, together with the precession frequency for part load conditions. This enables the prediction of the eigenfrequencies and resonance conditions of the full-scale generating unit.

1. Introduction

Hydraulic turbines operating in off-design conditions experience flow instabilities in their draft tube, promoting the onset of cavitation and the propagation of pressure fluctuations in the whole hydraulic circuit. In the worst cases, these can induce output power swings [1], mechanical vibrations and dynamic loads on the components of the machine [2].

In Francis turbines draft tube at part load conditions, i.e. with a discharge value lower than the value at the Best Efficiency Point (BEP), a cavitation vortex rope is observed at the runner outlet. The precession of this vortex with a frequency ranging from 0.2 to 0.3 times the runner frequency [3] induces the propagation of synchronous pressure pulsations at the same frequency and acts as a pressure excitation for the hydraulic circuit [4]. If the precession frequency matches with one of the eigenfrequencies of the hydraulic circuit, a hydro-acoustic resonance occurs [5][6], characterized by pressure pulsations of high amplitude and output power surges that jeopardize the stability of the whole system in the worst case. At full load, i.e. with a discharge value higher than the value at the BEP, the

axisymmetric cavitation vortex observed in the draft tube cone may auto-oscillate under certain conditions, inducing pressure and cavitation volume pulsations [7] [8].

The accurate prediction of the stability of hydropower plants and resonance conditions is essential to safely extend their operating range. For hydropower projects in an industrial context, the hydraulic behaviour of the machine is usually assessed by performing reduced scale physical model tests in laboratory. Even if similitude laws between model and prototype scales are fulfilled according to IEC International Standard [9], the pressure fluctuations cannot be directly transposed from the model to the prototype due to differences in terms of hydraulic circuit configuration. Therefore, one-dimensional (1D) hydro-acoustic models including the draft tube cavitation flow are used to predict and simulate resonance conditions, see Dörfler [4], Couston and Philibert [10] and Alligné et al. [11]. Alligné et al. [12] predicted the first eigenfrequency of a 444 MW full-scale generating unit at two different part load operating points. They transposed the hydro-acoustic parameters of the draft tube cavitation flow identified on the reduced scale model by Landry et al. [13].

In the present study, a methodology to predict the eigenfrequencies of hydropower plant units operating at both part load and full load is proposed and validated. The methodology is based on reduced scale physical model tests and 1D models of both the test rig at the model scale and the full-scale generating unit. The methodology is applied at part load conditions and enables the prediction of resonance conditions. At full load, it enables the prediction of the instability frequency, since the vortex rope enters self-oscillations at one of the first eigenfrequencies of the hydraulic circuit.

2. Reduced scale physical model test

A 1:16 reduced scale physical model of a Francis turbine with 16-blades and a specific speed of $\nu = 0.27$ is used as a test case, see Figure 1. Investigations of flow instabilities at deep part load, part load and full load conditions can be found in [14] [15][16] for the same test case. The reduced scale physical model is installed on the PF3 closed-loop test rig of the EPFL Laboratory for Hydraulic Machines, which enables performance tests of hydraulic machines within an accuracy better than 0.3 % according to IEC International Standard [9]. A set of dynamic pressure sensors is installed in one cross-section of the draft tube cone to decompose pressure fluctuations into convective and synchronous components [17]. Two additional sensors p_5 and p_6 are also placed in the upstream pipes of the machine to evaluate the hydro-acoustic response of the test rig.

At both part and full loads, pressure fluctuations measurements are performed within a wide range of discharge factor values for 4 different values of speed factor while the net head H and the Froude number $\mathrm{F} = (H / D)^{0.5}$ are kept constant. The Thoma number is set at the rated value corresponding to the average *NPSE*-value on the prototype. In addition, measurements in Froude similitude, i.e. with a Froude number corresponding to the value on the prototype, are also performed for several operating conditions. The investigated operating conditions are summarized in Figure 2.

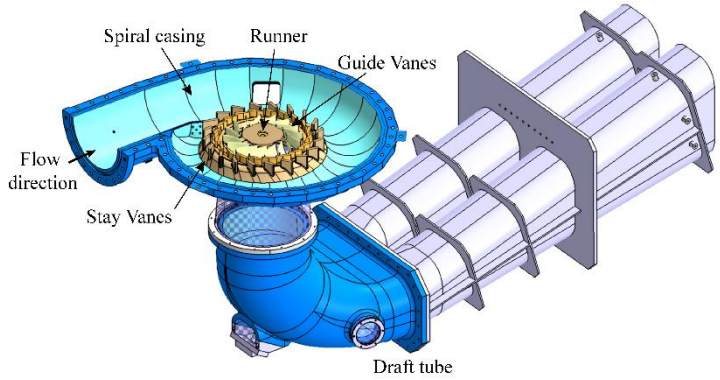

Figure 1. Components of the reduced scale physical model of a Francis turbine used for the present study

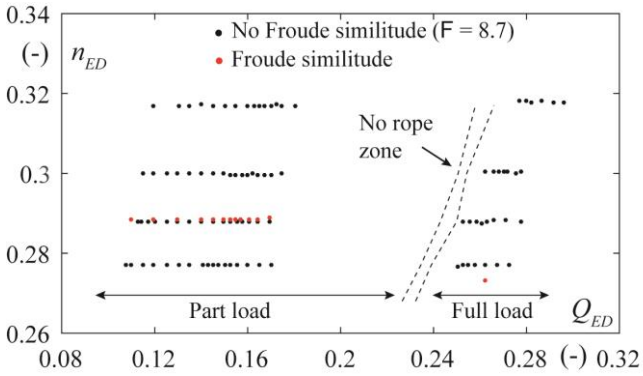

Figure 2. Investigated operating conditions

3. Experimental identification of the frequencies of interest during model tests

3.1. Identification of the precession frequency and first eigenfrequency at part load conditions

For a given operating point at part load, the precession frequency of the vortex rope and the first eigenfrequency of the test rig can be identified by simple spectral analysis of pressure signals measured in one section of the draft tube cone, as highlighted by Favrel et al. [18]. Both frequencies are identified for all the investigated operating points at part load.

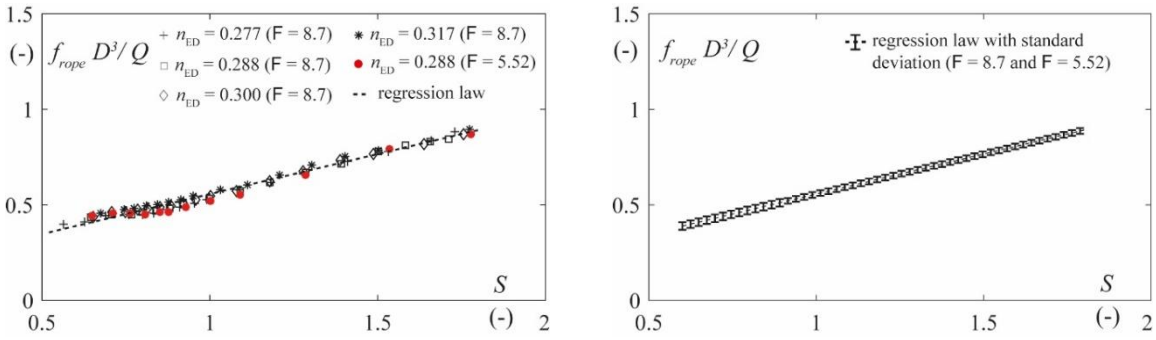

(a) Experimental data (b) Linear regression law

Figure 3. Strouhal number of the precession frequency as a function of the swirl number S computed according to [18] at part load conditions

Both speed and discharge factors influence the value of the precession frequency and the eigenfrequencies of the test rig. However, Favrel et al. [18] showed that the influence of both parameters can be represented by a single curve if the frequencies are plotted as a function of the swirl number, whose analytical expression as a function of the speed and discharge factors was derived [18].

The Strouhal number of the precession frequency is plotted as a function of the swirl number in Figure 3a. All the data, whatever the value of the speed factor and Froude number, collapse to one single curve, which can be represented by a linear regression law with corresponding standard deviation as given in Figure 3b. This curve can be therefore used to determine the precession frequency of the vortex on the complete operating range of the machine at part load, whatever the value of the Froude number.

The first eigenfrequency is also plotted as a function of the swirl number in Figure 4. The data with F = 8.7, i.e. without Froude similitude between prototype and model, collapse to one single curve, which can be represented by a power regression law with corresponding standard deviation as shown in Figure 4b. However, as shown in Figure 4a, the data at F = 5.52 draw a similar curve but with a slight shift, which highlights the influence of the Froude number on the eigenfrequencies of the test rig. In Section 4.2, the value of the first eigenfrequency is used to determine the hydro-acoustic parameters modelling the draft tube cavitation flow.

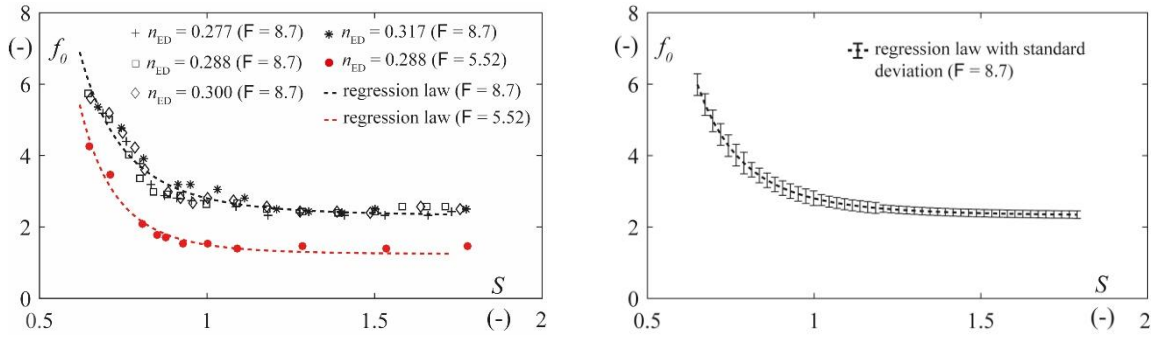

(a) Experimental data (b) Power regression law

Figure 4. First eigenfrequency of the hydraulic circuit as a function of the swirl number at part load

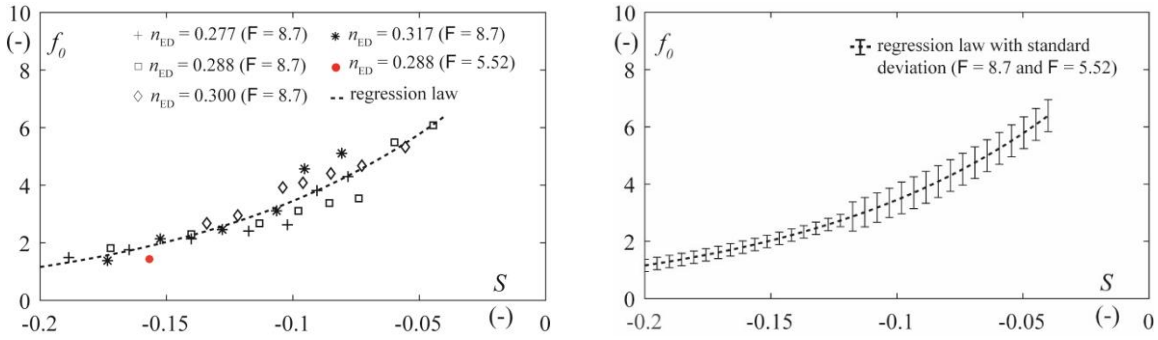

(a) Experimental data (b) Power regression law

Figure 5. First eigenfrequency of the hydraulic circuit as a function of the swirl number at full load

3.2. Identification of the first eigenfrequency at full load conditions

At full load, the vortex rope enters self-oscillations at the first eigenfrequency of the test rig under certain conditions of pressure level in the draft tube. Therefore, if the vortex rope is unstable, the first eigenfrequency of the test rig can be easily identified by spectral analysis of pressure fluctuations measured in the draft tube cone. The first eigenfrequency of the test rig is determined for all the investigated unstable operating points and plotted as a function of the swirl number in Figure 5a. Once again, all the data, including the one in Froude similitude, collapse to one single curve, whose power regression law with corresponding standard deviation is given in Figure 5b.

4. Identification of hydro-acoustic parameters modelling the draft tube flow at the model scale

In the following, the hydro-acoustic parameters modelling the draft tube cavitation flow are determined for all the investigated operating points by using the value of the first eigenfrequency and a 1D hydro-acoustic model of the test rig. First, a brief description of the hydro-acoustic modelling of the draft tube cavitation flow is provided.

4.1. Hydro-acoustic modelling of draft tube cavitation flow

SIMSEN software is used [19] to model both the test rig at the model scale and the hydropower plant generating unit. For the modelling of the draft tube cavitation flow, the model proposed by Alligné et al. [11] is considered. It takes into account the divergent geometry of the draft tube and the convective terms of the momentum equation. Details about the modelling of draft tube cavitation flows can be found in Alligné et al. [11] and Landry et al. [13].

An additional dissipation is modelled in the electrical T-shaped circuit by a hydraulic resistance R_μ:

$$R_\mu = \frac{\mu''}{\rho_w g A \mathrm{d}x} \tag{1}$$

where μ'' is the bulk viscosity, ρ_w is the water density, A and dx are the section and the length of the pipe element, respectively, and g is the gravity acceleration.

The development of cavitation in the draft tube induces an additional compressibility modelled by the cavitation compliance Cc [20]. It represents the variation of the cavitation volume with respect to the pressure as follows:

$$Cc = -\frac{\partial Vc}{\partial h} \tag{2}$$

where h is the piezometric head. The equivalent compliance C_{eq} of the draft tube, including the wall, the water and the cavitation volume, is directly linked to the local wave speed a in the draft tube and is expressed as follows:

$$C_{eq} = (1-\beta)C_0 + Cc = \frac{gAdx}{a^2} \tag{3}$$

where β is the void fraction, i.e. the ratio between the cavitation volume and the total volume of the draft tube, and C_0 is the compliance of the draft tube without cavitation. In cavitation conditions, the compliance of both the draft tube wall and the water volume can be neglected [13], which finally leads to:

$$Cc \approx \frac{gAdx}{a^2} \tag{4}$$

The momentum excitation source induced by the vortex precession is taken into account in the 1D numerical model by introducing an additional momentum source S_h. The hydro-acoustic parameters modelling the cavitation vortex rope, i.e. the bulk viscosity μ'', the local wave speed a and the momentum excitation source S_h, remain unknown and need to be identified experimentally. In the following, only the wave speed and the bulk viscosity are identified since the pressure source does not influence the eigenfrequencies of the hydraulic circuit.

4.2. Identification of hydro-acoustic parameters based on the value of the first eigenfrequency

Landry et al. [13] used an excitation system to identify the first eigenfrequency of the hydraulic circuit and its hydro-acoustic response for several operating points at part load conditions. Based on the experimental results, the wave speed and the bulk viscosity are calibrated in the 1D model of the test rig. They considered a distributed cavitation compliance in the Francis turbine draft tube. Two dimensionless numbers, the dimensionless wave speed Π and the dimensionless bulk viscosity M'', are defined as follows [13]:

$$\Pi = \frac{\rho_w a^2}{p_{cone} - p_v} \tag{5}$$

$$\mathrm{M}'' = \frac{\mu'' f_0}{p_{cone} - p_v} \tag{6}$$

where p_{cone} is the mean pressure in a reference section of the draft tube cone and f_0 is the first eigenfrequency of the hydraulic circuit. By plotting these dimensionless parameters as a function of the void fraction β in the draft tube, all the data collapse in single curves that can be approximated by single power functions. These are valid whatever the value of speed factor, discharge factor, Thoma number and Froude number. In the present study, no excitation system is used and only the value of the first

eigenfrequency is known for a given operating point. The wave speed and the bulk viscosity are identified by procedure coupling the 1D model of the test rig and the dimensionless law $\Pi = f(\beta)$ and $M^{''} = f(\beta)$ defined in [13], see [21] for more details.

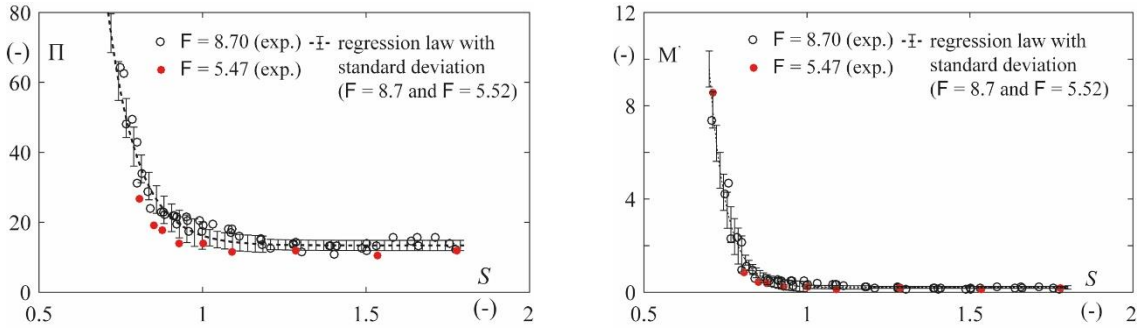

(a) Dimensionless wave speed (b) Dimensionless bulk viscosity

Figure 6. Dimensionless hydro-acoustic parameters as a function of the swirl number at part load

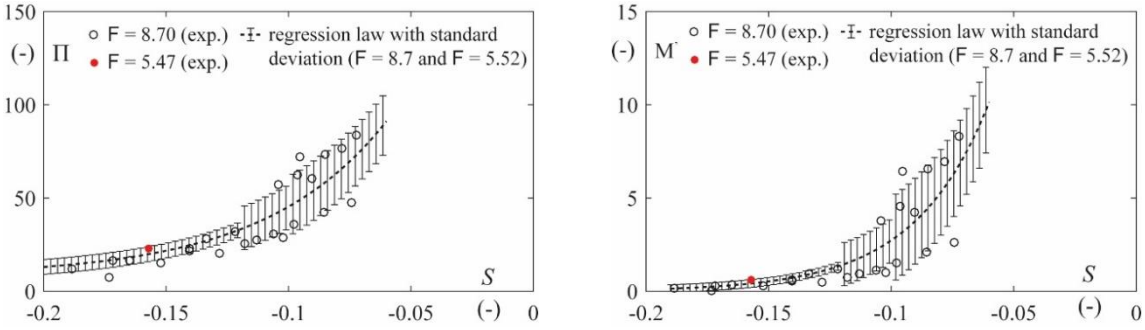

(a) Dimensionless wave speed (b) Dimensionless bulk viscosity

Figure 7. Dimensionless hydro-acoustic parameters as a function of the swirl number at full load

The dimensionless hydro-acoustic parameters, as defined by Equation 5 and Equation 6, are determined at both part load and full load for all the investigated operating points. The results are plotted as a function of the swirl number at part load and full load in Figure 6 and Figure 7, respectively. At part load, the data collapse to one single curve, whatever the value of the Froude number, for both dimensionless wave speed and bulk viscosity. The resulting curves can be represented by regression power laws with the corresponding standard deviation. Therefore, these dimensionless laws represent the influence of the speed factor, discharge factor and Froude number on the dimensionless hydro-acoustic parameters for a given Thoma number. Similar behaviour is found at full load, see Figure 7, with however a higher standard deviation for the values of swirl number between S = -0.12 and S = -0.06. Indeed, this operating regime corresponds to the onset of the full load instability, which is very sensitive to operating conditions and can vary because of different gas rates in the water for instance.

5. Prediction of eigenfrequencies at the prototype scale and validation by on-site tests

5.1. On-site tests for validation

Measurements are performed on the corresponding 444 MW full-scale generating unit located in Canada.

Table 1. Investigated operating conditions during prototype tests

OP	P / P_{rated} (-)	n_{ED} (-)	Q_{ED} (-)	F (-)	σ (-)	S (-)	Comment
1	1.07	0.2787	0.2533	5.72	0.1176	-0.09	Full load
2	0.70	0.2763	0.1632	5.77	0.1021	0.64	Part load
3	0.66	0.2763	0.1556	5.77	0.1024	0.75	Part load
4	0.61	0.2764	0.1439	5.76	0.1038	0.92	Part load
5	0.59	0.2765	0.1406	5.76	0.1045	0.98	Part load
6	0.57	0.2764	0.1361	5.76	0.1036	1.06	Part load
7	0.54	0.2763	0.1302	5.76	0.1033	1.17	Part load
8	0.51	0.2763	0.1237	5.76	0.1036	1.31	Part load
9	0.48	0.2759	0.1188	5.77	0.1008	1.42	Part load

Pressure measurements are performed in the water passages of the machine, including the draft tube cone, the spiral case and the penstock, at 9 different values of output power at both full load and part load. The output electrical power P, headwater level HWEL, tailwater level TWEL and opening angle of the guide vanes α, are also measured during the tests. The operating parameters of the machine, including the speed factor, the discharge factor and the Thoma number, can be estimated based on a model for the losses. The model of the turbine efficiency η_h as a function of the discharge Q and the net head H_{net} is based on experimental data measured during reduced scale model tests, as described in Andolfatto et al. [22]. The corresponding operating parameters are given in Table 1.

5.2. Transposition of the hydro-acoustic parameters from model to prototype

For each operating point measured on the prototype, the corresponding swirl number is computed by using the analytical expression derived in [18]. The corresponding dimensionless hydro-acoustic parameters can be determined by using the dimensionless laws defined in Figure 6 and Figure 7. By knowing the pressure level in the cone, which is measured by 3 pressure sensors located in the same cross-section of the cone, the wave speed at the prototype scale can be directly computed. However, the transposition of the bulk viscosity requires the value of the first eigenfrequency, see Equation 6. Therefore, the value of the bulk viscosity, together with the first eigenfrequency of the prototype, must be computed by using the algorithm given in Figure 8.

5.3. Prediction of resonance at part load conditions

At part load conditions, the precession frequency of the vortex can be predicted at the prototype scale by transposing directly the empirical law defined at the model scale and given in Figure 3b. The first eigenfrequency of the hydropower generating unit is predicted for the operating points tested during on-site measurements by using the procedure described in the previous section. The predicted values of frequency, together with the values identified during on-site tests, are given in Figure 9. It is worth to precise that the first eigenfrequency of the hydropower generating unit can be identified during on-site tests by performing simple spectral analysis of pressure fluctuations measured in the draft tube cone, similarly to model tests.

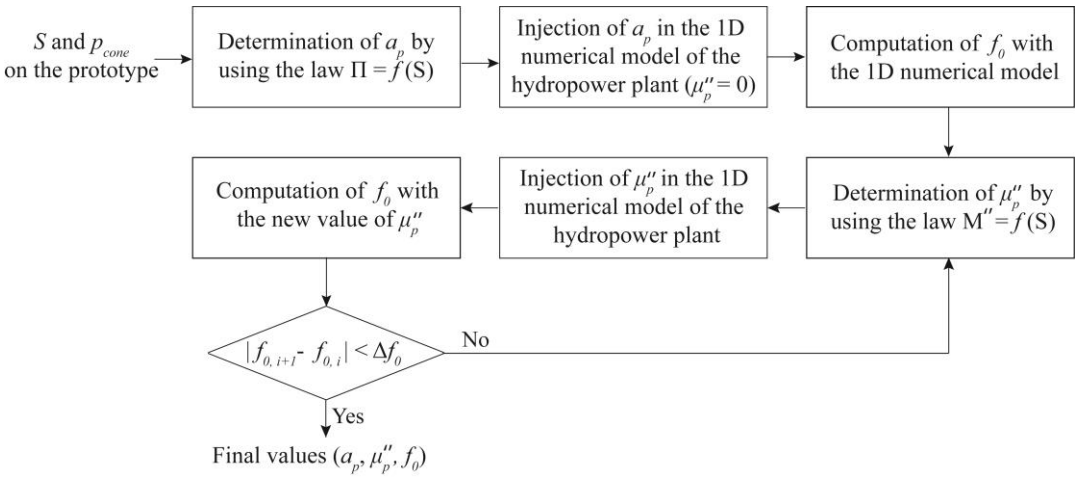

Figure 8. Procedure for computation of the bulk viscosity and the first eigenfrequency at the prototype scale for a given operating point

For the precession frequency, an excellent agreement is observed between predicted and experimental results. At $P = 0.66 \times P_{rated}$, the deviation is equal to $0.02 \times n$, which represents only 9 % of the predicted value. All the other experimental values are in the range of uncertainty of the predicted values.

For the first eigenfrequency of the prototype, the predicted values feature similar shape to the experimental ones. However, a clear difference is observed between prediction and experiments. The difference ranges from $0.01 \times n$ at $P = 0.70 \times P_{rated}$ to $0.11 \times n$ at $P = 0.59 \times P_{rated}$, which corresponds to 2 % and 33 % of the predicted values, respectively. As shown in Figure 9, the resonance is observed during on-site tests at $P \approx 0.57 \times P_{rated}$ whereas the methodology predicts the occurrence of resonance at $P \approx 0.62 \times P_{rated}$, which corresponds to a shift equal to 5 % of the rated output power of the machine. However, similitude in terms of local cavitation coefficient in the draft tube cone is not achieved between model and prototype for the present test case even if Thoma numbers are similar. This might cause a discrepancy in terms of local wave speed in the draft tube cone and explain the shift between predicted and experimental values.

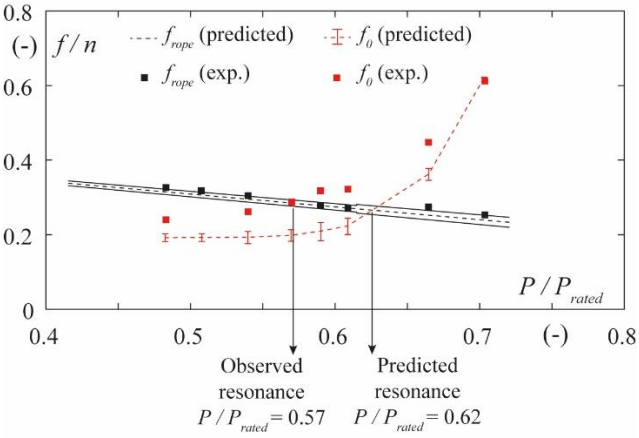

Figure 9. Predicted and measured frequencies at the prototype scale in part load conditions

5.4. Prediction of full load instability frequency

Only one operating point at full load is investigated during on-site tests. At this point, the cavitation vortex rope enters self-oscillations, leading to strong pressure pulsations in the whole hydraulic circuit of the generating unit, as reported in [8]. The frequency of the instability is determined by spectral analysis of the pressure fluctuations and is equal to $f_0 / n = 0.37$.

The first eigenfrequency of the generating unit, which corresponds to the frequency of the instability, is predicted for this operating point by using the methodology presented previously. The predicted value is equal to $f_0 / n = 0.33 \pm 0.06$. Contrary to the results at part load, the predicted value is in very good agreement with the experimental one: the latter is comprised within the range of uncertainty of the predicted value.

6. Conclusion and discussion

The first eigenfrequency of a hydropower plant unit with a conventional Francis turbine operating at part load and full load, as well as the precession frequency of the vortex rope at part load, are predicted on the complete operating range based on a new approach.

To predict the first eigenfrequency of the prototype, the hydro-acoustic parameters modelling the draft tube cavitation flow are identified by coupling experimental data measured on the corresponding reduced scale physical model and 1D hydro-acoustic models of both the test rig at the model scale and the hydropower plant unit. Empirical laws linking dimensionless hydro-acoustic parameters and the swirl number are then defined, enabling the prediction of their value on the complete operating range of the machine, whatever the value of discharge factor, speed factor and Froude number. Such empirical laws are however valid for one given value of Thoma number. In addition, an empirical law linking the precession frequency of the part load vortex and the swirl number is defined at the model scale. It represents the influence of both the discharge and speed factors on its value, whatever the Froude number, by a simple linear regression law. The value of the precession frequency can be predicted on the complete part load operating range of the full-scale machine by directly transposing the empirical law established at the model scale.

The predicted values are finally compared with experimental results measured on the full-scale machine. At part load, a slight discrepancy between the predicted resonance conditions and the ones identified during prototype tests is observed. However, similitude in terms of local cavitation coefficient in the draft tube cone is not achieved between model and prototype for the present test case even if Thoma numbers are similar. This induces differences between the predicted values of local wave speed and the ones observed on the prototype, and therefore differences in terms of eigenfrequencies. A perfect agreement is however found between prediction and measurements for the precession frequency. Finally, a good agreement is observed at full load between predicted and observed values of the first eigenfrequency of the prototype.

The methodology presented in this paper represents a decisive step towards the stability assessment of hydropower plants and the prediction of pressure pulsations on the complete operating range, which is the ultimate challenge. The methodology is applicable in an industrial context, which represents a decisive contribution to the stability assessment of hydropower plants in the course of new renewable energy integration. It might lead in the future to the revision of the scale-up relating to oscillating phenomena in the IEC 60193 Standard for industrial model testing.

Acknowledgments

The research leading to the results published in this paper is part of the HYPERBOLE research project, granted by the European Commission (ERC/FP7-ENERGY-2013-1-Grant 608532). The authors would like to thank BC Hydro (CA) for making available the reduced scale model, in particular Danny Burggraeve and Jacob Iosfin. Moreover, the authors would like to acknowledge the commitment of the Laboratory for Hydraulic Machines' technical staff, especially Raymond Fazan, Georges Crittin, Alain Renaud and Vincent Berruex, and the HYPERBOLE partners involved in the on-site tests.

References

[1] Rheingans W 1940 *Transactions of the ASME* **62** 171-184
[2] Lowys P, Andre F, Ferreira da Silva A, Duarte F and Payre J.-P 2014 *Proceedings of Hydrovision*, *Nashville, USA*
[3] Arpe J, Nicolet C and Avellan F 2009 *Journal of Fluids Engineering* **131**(8)

[4] Dörfler P 1982 *Proceedings of the 11th IAHR Symposium on Operating Problem of Pump Stations and Powerplants, Amsterdam, Netherlands*
[5] Favrel A, Landry C, Müller A, Yamamoto K and Avellan F 2014 *IOP Conference Series: Earth and Environmental Science* **22**
[6] Fritsch A and Maria D 1988 *Houille Blanche* **3**(3-4) 273-281
[7] Müller A, Favrel A, Landry C and Avellan F 2017 *Journal of Fluids and Structures* **69** 56-71
[8] Valentin D, Presas A, Egusquiza E, Valero C, Egusquiza M and Bossio M 2017 *Energies* **10**
[9] IEC Standards, 60193: hydraulic turbines, storage pumps and pump-turbines - model acceptance tests (second edition) 1999 International Commission
[10] Couston M and Philibert R 1998 *The International Journal on Hydropower and Dams* **1** 146-158
[11] Alligné S, Nicolet C, Tsujimoto Y and Avellan F 2014 *Journal of Hydraulic Research* **52**(3)
[12] Alligné S, Landry C, Favrel A, Nicolet C, Avellan F 2015 *Journal of Physics: Conference Series* **656**(1)
[13] Landry C, Favrel A, Müller A, Nicolet C and Avellan F 2016 *Journal of Hydraulic Research* **54**(2)
[14] Yamamoto K, Müller A, Favrel A and Avellan F 2017 *Experiments in Fluids* **58**(10)
[15] Favrel A, Müller A, Landry C, Yamamoto K and Avellan F 2015 *Experiments in Fluids* **56**(12)
[16] Müller A, Dreyer M, Andreini N and Avellan F 2013 *Experiments in Fluids* **54**(4)
[17] Duparchy A, Guillozet J, De Colombel T and Bornard L 2014 *IOP Conference Series: Earth and Environmental Science* **22**
[18] Favrel A, Gomes Pereira Junior J, Landry C, Müller A, Nicolet C and Avellan F 2017 *Journal of Hydraulic Research* Published on-line
[19] Nicolet C 2007 *Hydroacoustic modelling and numerical simulation of unsteady operation of hydroelectric systems* Ph.D. thesis, EPFL, Lausanne, Switzerland
[20] Brennen C and Acosta A 1976 *Journal of Fluids Engineering, Transactions of the ASME,* **98** Ser 1(2)
[21] Favrel A, Gomes Pereira Junior J, Landry C, Alligné S, Andolfatto L, Nicolet C and Avellan F 2018 *Journal of Hydraulic Research* Under review
[22] Andolfatto L, Delgado J, Vagnoni E, Münch-Alligné C and Avellan F 2015 *E-Proceeding of the 36th IAHR World Congress 2015, La Hague, Netherlands*